Cross-Subject Motor Imagery Decoding by Transfer Learning of Tactile ERD

Yucun Zhong, Lin Yao, Gang Pan, *Senior Member, IEEE*, and Yueming Wang

***Abstract*— For Brain-Computer Interface (BCI) based on motor imagery (MI), the MI task is abstract and spontaneous, presenting challenges in measurement and control and resulting in a lower signal-to-noise ratio. The quality of the collected MI data significantly impacts the cross-subject calibration results. To address this challenge, we introduce a novel cross-subject calibration method based on passive tactile afferent stimulation, in which data induced by tactile stimulation is utilized to calibrate transfer learning models for cross-subject decoding. During the experiments, tactile stimulation was applied to either the left or right hand, with subjects only required to sense tactile stimulation. Data from these tactile tasks were used to train or fine-tune models and subsequently applied to decode pure MI data. We evaluated BCI performance using both the classical Common Spatial Pattern (CSP) combined with the Linear Discriminant Analysis (LDA) algorithm and a state-of-the-art deep transfer learning model. The results demonstrate that the proposed calibration method achieved decoding performance at an equivalent level to traditional MI calibration, with the added benefit of outperforming traditional MI calibration with fewer trials. The simplicity and effectiveness of the proposed cross-subject tactile calibration method make it valuable for practical applications of BCI, especially in clinical settings.**

***Index Terms*— Brain-Computer Interface (BCI), cross-subject decoding, motor imagery (MI), tactile ERD, tactile stimulation.**

Manuscript received 28 August 2023; revised 8 December 2023; accepted 12 January 2024. Date of publication 25 January 2024; date of current version 5 February 2024. This work was supported in part by STI 2030—Major Projects under Grant 2021ZD0200400, in part by the National Natural Science Foundation of China under Grant 62336007, in part by the Key Research and Development Program of Zhejiang under Grant 2023C03003, in part by the Starry Night Science Fund of the Zhejiang University Shanghai Institute for Advanced Study under Grant SN-ZJU-SIAS-002, in part by the Fundamental Research Funds for the Central Universities, in part by the Project for Hangzhou Medical Disciplines of Excellence, and in part by the Key Project for Hangzhou Medical Disciplines. *(Corresponding author: Lin Yao.)*

This work involved human subjects or animals in its research. Approval of all ethical and experimental procedures and protocols was granted by the Ethics Committee of Zhejiang University.

Yucun Zhong is with the Department of Neurobiology, Affiliated Mental Health Center & Hangzhou Seventh People's Hospital, Zhejiang University School of Medicine, Hangzhou 310058, China, also with the Nanhu Brain-Computer Interface Institute, Hangzhou 311100, China, also with the MOE Frontiers Science Center for Brain and Brain-Machine Integration, Zhejiang University, Hangzhou 310027, China, and also with the College of Computer Science, Zhejiang University, Hangzhou 310027, China.

Lin Yao is with the Department of Neurobiology, Affiliated Mental Health Center and Hangzhou Seventh People's Hospital, Zhejiang University School of Medicine, Hangzhou 310058, China, also with the Nanhu Brain-Computer Interface Institute, Hangzhou 311100, China, and also with the MOE Frontiers Science Center for Brain and Brain-Machine Integration, the College of Computer Science, and the College of Biomedical Engineering and Instrument Science, Zhejiang University, Hangzhou 310027, China (e-mail: lin.yao@zju.edu.cn).

Gang Pan is with the College of Computer Science and Technology and the First Affiliated Hospital, State Key Laboratory of Brain-Machine Intelligence, Zhejiang University, Hangzhou 310027, China.

Yueming Wang is with the Qiushi Academy for Advanced Studies, the Nanhu Brain-Computer Interface Institute, and the College of Computer Science and Technology, Zhejiang University, Hangzhou 310027, China.

Digital Object Identifier 10.1109/TNSRE.2024.3358491

I. Introduction

BRAIN-COMPUTER Interface (BCI) establishes a direct communication and control pathway between the brain and the external environment [1]. For individuals with amyotrophic lateral sclerosis (ALS) who experience severe communication and physical limitations, BCI represents a valuable tool. By enabling interaction with the external world, BCI offers a means for these patients to enhance their quality of care and engagement with the environment [2]. Electroencephalography (EEG) is one of the most widely used brain signals in BCI, due to its safety and convenience [3]. Compared to visual P300 [4] and steady-state visual evoked potentials (SSVEP) [5], which rely on external visual stimuli, motor imagery (MI) [6] is completely spontaneous and not dependent on external visual stimuli. This paper specifically focuses on BCIs that are based on motor imagery. MI-based BCI detects event-related (de)synchronization (ERD/ERS) patterns that are induced when users imagine performing kinesthetic movements of different body parts, such as the left hand or right hand, and subsequently translate these patterns into instructions. Due to the intrinsic relationship between motor imagery and actual physical movement, MI-based BCI has gained significant attention and is extensively employed in the field of stroke neurorehabilitation [7], [8].

However, the widespread adoption of MI-based BCI has been hindered by certain challenges, with one major obstacle being the calibration process required prior to actual online usage [9]. The typical MI-based BCI system consists of a calibration phase and a testing phase [10]. During the calibration phase, EEG data is collected to train a classification model, while in the testing phase, MI tasks are decoded using the calibrated model. Due to the non-stationarity [11] and the low signal-to-noise ratio [12] of EEG signals, a substantial amount of calibration data is required to obtain a more accurate classifier during the calibration phase. This requirement significantly diminishes the user experience, particularly for

patients in clinical applications where long-term calibration data collection is not convenient.

To reduce the calibration effort and improve the quality of calibration data, one approach is to explore alternative methods for inducing calibration data to the traditional MI data. In the traditional MI calibration method, users are required to perform MI tasks in both the calibration and testing phases [13]. However, the calibration phase lacks feedback, and users need to repeat MI tasks without clear instructions, which can impose a heavy cognitive burden [14]. Additionally, some users may struggle to generate clear patterns of event-related desynchronization (ERD) initially [2], posing challenges for accurate decoding by the classification model [13], which can lead to calibration failure. Moreover, MI is an abstract and implicitly performed task, making it difficult to ensure that users are executing the MI task correctly. To address these challenges, researchers have proposed alternative methods to the traditional MI calibration approach. Studies have shown that both active and passive movements can elicit brain patterns similar to MI [15]. Brain patterns induced by passive movements [16] and functional electrical stimulation [17] have been utilized for MI calibration. However, passive movement calibration requires the assistance of a robot, which presents implementation challenges and may not be well-suited for clinical applications. Additionally, electrical stimulation can introduce artifacts that lower the signal-to-noise ratio of the EEG [18]. Therefore, while these alternative methods show promise, there are practical limitations that need to be considered in their application.

Another commonly employed approach to reduce the calibration effort is transfer learning [19], which involves leveraging information from other domains (subjects/sessions) [20], [21], [22] or even other datasets [23], [24] to improve calibration performance in the target domain. Numerous recent studies have demonstrated the effectiveness of traditional transfer machine learning methods in BCI [21], [25], [26]. Many researchers have extended the classical Common Spatial Pattern (CSP) algorithm by incorporating kernel techniques [27], [28] or regularized terms [29], [30] to find domain-invariant CSP filters. Another approach involves aligning the data between the source and target domains based on the covariance matrices of EEG trials [31], [32], [33], such as Riemannian alignment [33] or Euclidean alignment [34]. Additionally, transfer learning methods based on deep neural networks have also shown significant potential [35], [36], [37]. Pérez-Velasco et al. proposed the EEGSym model [38], which facilitates knowledge transfer across datasets and reaches state-of-the-art performance in cross-subject decoding scenarios. The success of transfer learning hinges on identifying common patterns across different domains [39]. However, a challenge lies in the inherent weaknesses of motor imagery patterns [39], which result in a decrease in the signal-to-noise ratio of the EEG signals [12] and an increase in the variability of these patterns across subjects [40], [41]. In the context of cross-subject decoding, previous research has primarily concentrated on algorithm design [19]. However, recent advancements in the field of Artificial Intelligence (AI) have brought attention to the significance of shifting research focus from a model-centric approach to a data-centric approach [42], with an increased emphasis on acquiring higher quality data [42]. Therefore, how to obtain more distinct EEG patterns may be a crucial factor in enhancing performance in BCI.

Tactile stimulation has gained considerable traction in recent years as a widely utilized approach within BCI systems to enhance BCI applications [43], [44], [45]. Tactile-induced brain patterns were used to construct new BCI paradigms, such as selective sensation BCIs [46], tactile P300 BCIs [43], and hybrid BCIs with MI [47]. During the process of actual movement, sensory interaction with the environment is also a crucial component, where movement and sensation are considered to be a unified entity [48]. However, sensory interaction might be absent in motor imagery. Many researchers have suggested using tactile stimulation as a means to compensate for the absence of sensory interaction and proposed several approaches as tactile feedback of MI [45], tactile assisted MI training [49], and tactile MI guidance [50]. Interestingly, in our previous study [51], we found that tactile stimulation can also induce brain patterns similar to that induced by MI. As a form of passive input, tactile stimulation offers several advantages over abstract MI tasks. It provides a more explicit and controllable means of eliciting brain patterns, making it a potentially promising approach for calibrating MI-based BCI systems in the cross-subject scenario. However, the suitability of utilizing brain patterns induced by tactile stimulation for cross-subject motor imagery decoding remains to be verified.

In this study, we proposed a cross-subject calibration method based on tactile stimulation. We hypothesized that the MI-based BCI could be calibrated using the brain patterns elicited by tactile stimulation in the cross-subject calibration scenario. A high-density EEG device was used to obtain EEG signals, and we compared the brain patterns induced by tactile stimulation and MI in both the spatial and frequency domains. We compared the proposed calibration method with the traditional MI calibration method. The performance of our calibration method has been verified using both the classical Common Spatial Pattern (CSP) algorithm [52] and one of the state-of-the-art deep transfer learning algorithms [38]. To our knowledge, this is the first study to explore the utilization of tactile input in the cross-subject decoding scenario.

II. Materials and Methods

A. Subjects

A total of 12 subjects (6 males and 6 females, with an average age of 23.5 $\pm$ 1.6 years old) participated in the experiment. Ten of these subjects participated motor imagery experiment once, but they were all naive to tactile stimulation. They were right-handed and in self-reported good health condition, and they all signed an informed consent form before participation. This study was permitted by the Ethics Committee of Zhejiang University, Zhejiang, China.

B. EEG Recording and Stimulation Device

EEG signal was recorded with the BioSemi ActiveTwo EEG amplifier (BioSemi Inc., Amsterdam, the Netherlands) from a high-density (128-channel) active head cap, whose

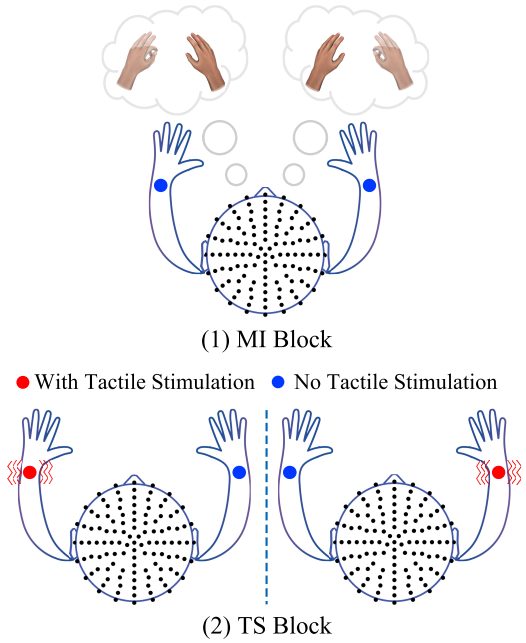

Fig. 1. Graphic illustration of the experimental paradigm. (1) is the MI block, in which the subjects performed the MI-L and the MI-R tasks with two runs, and (2) is the TS block, in which the subjects performed the TS-L and the TS-R tasks with two runs. The red circle on the wrists indicates that the tactile stimulation motor is on, and the blue circle indicates the tactile stimulation motor is off.

electrodes were positioned according to the BioSemi ABC position system. The Common Mode Sense (CMS) active electrode served as reference and the Driven Right Leg (DRL) passive electrode served as ground. Additional two active electrodes were placed at the left and right mastoids for re-references. During the whole recording process, the magnitude of the offset of all electrodes to the CMS electrode was kept between ±25 mV, and the signals were sampled at 512 Hz.

The tactile stimulation was generated by two linear resonant actuators (vibrotactile stimulators, 10 mm, C10-100, Precision Microdrives Ltd., typically normalized amplitude 1.4 G), which were attached on the dorsal side of the subject's left wrist and the right wrist. The Pacinian corpuscles and the Meissner corpuscles are two kinds of tactile receptors, and they are sensitive to mechanical stimuli of above 100 Hz and 20-50 Hz, respectively [53]. Thus, the tactile stimulation frequency was set as 27 Hz with a sine wave modulated by a 175 Hz sine carrier wave to activate both types of the two receptors. The vibration amplitude could be adjusted according to the feedback of the subjects, and they all reported that they were comfortable with perceiving the vibration.

C. Experimental Paradigm

This experimental paradigm consisted of a motor imagery (MI) block and a tactile stimulation (TS) block. During the MI block, MI tasks were performed, in which the subjects mentally simulated kinesthetic movements of either their left or right hand without any actual physical movement. During the TS block, tactile stimulation tasks were performed, in which the tactile stimulation was applied to either their left or right wrist, and the subjects were required to perceive the stimulation. In each block, there were two runs, and each run consisted of 40 trials. There were a total of 160 trials for each subject. Subjects had a self-controlled rest period of 1∼2 minutes between runs and blocks. Before the start of the experiment, the subjects were fully familiar with the experimental procedure and were given a practice session consisting of about 30 trials.

1) Motor Imagery (MI) Block: The experiment was carried out in a noise-shielded room. A 14 × 24-inch screen with a black background was used for presenting instructions. The subjects sat in a comfortable chair and rested their hands on the armrest. They were allowed to adjust the height of the computer desk and chair to ensure their comfort during the experiment. Throughout the experiment, the subjects were required to avoid any facial and hand muscle movements and to limit blinking while performing the task. The whole experiment was monitored by an experimenter to ensure that the subjects followed the instructions correctly. At the beginning of each trial (T = 0 s), a white cross appeared in the center of the screen, and the subjects began to prepare for the MI task and kept their eyes focused ahead. At T = 2 s, the vibrotactile stimulators on both wrists simultaneously gave a burst vibration for 200 ms to alert the subjects that the MI task was about to start. At T = 3 s, a red square cue appeared on the left or right side, overlapping on the white cross. When the cue appeared on the left or right side, the subject started to perform the left or right MI (MI-L or MI-R) task, respectively, lasting for 5 s until the white cross disappeared at T = 8 s. Note, the cue only lasted for 1.5 s and disappeared at T = 4.5 s. After the cross disappeared, the subjects had a rest time of 1.5∼3.5 s before the start of the next trial to prevent fatigue and limit adaptation. In this block, a total of two runs were conducted, each consisting of 20 trials for the MI-L task and 20 trials for the MI-R task, resulting in a total of 80 trials.

2) Tactile Stimulation (TS) Block: The only difference between this block and the MI block was that the subjects performed different tasks, and the timeline and other settings of this block were the same as the MI block. In this block, the subjects performed the tactile stimulation tasks rather than the MI tasks. When the cue appeared on the left or right side, the tactile stimulation was applied to the left or right wrist, respectively, and the subjects were required to perform the left- or right-hand tactile stimulation (TS-L or TS-R) task, perceiving the tactile stimulation on the corresponding hand. Note, that in each trial of the TS block, the tactile stimulation was applied only on one side (either left or right) corresponding to the side where the cue appeared. The tactile stimulation lasted for 5 s, starting from the appearance of the cue. In this block, a total of two runs were conducted, each consisting of 20 trials for the TS-L task and 20 trials for the TS-R task, resulting in a total of 80 trials.

D. Calculation of EEG Dynamics

A custom MATLAB script and EEGLAB were used to preprocess the raw signals according to a standard process pipeline [54]. Firstly, the raw signals were re-referenced to the common average and then filtered using a second order, Butterworth, zero-phase shift [8 26] Hz band pass filter. Then,

highly contaminated artifacts were removed by visual inspection. Thereafter, an independent component analysis (ICA) was performed to further remove artifacts, such as ocular and muscle artifacts.

The widely recognized physiological characteristics of motor imagery (MI) are event-related desynchronization (ERD) and event-related synchronization (ERS), which are described as changes in power in a particular frequency band relative to a baseline period [6]. Prior to calculating the power changes, time-frequency decomposition was performed by EEGLAB toolbox [54], utilizing a hamming taper window (with a window length varying linearly with frequency and a time step of 350 milliseconds). For each trial, the ERD/ERS was calculated by subtracting the average power of the baseline period (from 2 s to 1.2 s before the red cue bar appeared) from the task-performing period. Then, the grand-averaged ERD/ERS was calculated by taking the average of all the trials across all subjects. Moreover, in order to demonstrate the discriminative information between tasks, we also computed the square of the Pearson correlation coefficient of the powers and task class labels (i.e. R^2). Subsequently, the grand-averaged R^2 was also determined by computing the average of R^2 values across all subjects. The ERD/ERS and R^2 were compared between the motor imagery (MI) task and the tactile stimulation (TS) task.

E. Algorithms and Performance Evaluation

1) Data Alignment in the Euclidean Space: In order to achieve data distribution alignment across different subjects and tasks (i.e. MI and TS), we initially employed a transfer learning technique, specifically Euclidean Alignment [34], to map the data from various subjects and tasks onto a shared data space. Specifically, each MI trial X_i was transformed by:

$$X_i' = M_{MI}^{-1/2} X_i \tag{1}$$

where M_{MI} is the Euclidean mean of the covariance matrices of all MI trials. For each TS trial X_i, it was transformed by:

$$X_i' = M_{TS}^{-1/2} X_i \tag{2}$$

where M_{TS} is the Euclidean mean of the covariance matrices of all tactile stimulation trials. It should be noted that the Euclidean mean M_{MI} and M_{TS} were separately calculated for each subject, and in the above equations, the trial and the Euclidean mean came from the same subject.

2) Common Spatial Pattern: In the CSP-LDA algorithm, we used the classical Common Spatial Pattern (CSP) algorithm [55] as the feature extractor and the Linear Discriminative Analysis (LDA) algorithm as the classifier. In MI-based BCI, the discriminative information and common information between the two classes can be described as the difference and the sum of the covariance respectively:

$$\begin{aligned} S_d &= \Sigma^{(l)} - \Sigma^{(r)} \\ S_c &= \Sigma^{(l)} + \Sigma^{(r)} \end{aligned} \tag{3}$$

$\Sigma^{(l)}$ represents the covariance of the left hand task, $\Sigma^{(r)}$ represents the covariance of the right hand task. CSP finds directions, which maximize the discriminative information and minimize the common information at the same time by:

$$\begin{aligned} &\underset{w}{\text{maximize}} \quad \frac{w^\top S_d w}{w^\top S_c w} \\ &\text{s.t.} \quad w^\top S_c w = 1 \end{aligned} \tag{4}$$

Through the Lagrange multiplier method, the objective function can be transformed into the generalized eigenvalue problem:

$$S_d w = \lambda S_c w \tag{5}$$

For the eigenvector w, it satisfies:

$$w\Sigma^{(l)} w + w\Sigma^{(r)} w = 1 \tag{6}$$

In other words, in the direction, w, the sum of the variance of the two classes is 1. Therefore, when the projection direction maximizes the variance of one class, it simultaneously minimizes the variance of the other class at the same time. We selected three directions to maximize the variance of the MI-L task and the TS-L task, and another three directions to maximize the variance of the MI-R task and the TS-R task. After projecting the data to the six directions, the variance of the projected data was logarithmically transformed to obtain six CSP features. Thereafter, we used the LDA algorithm for classification.

3) Cross-Subject Decoding: To decode the data from one subject, the data from all other subjects were used as calibration data. The subject under consideration for decoding was designated as the target subject, while all the remaining subjects were referred to as the source subjects.

In the aligned data space, the calibration performance was evaluated by two algorithms. The first algorithm is CSP-LDA, which was previously introduced. According to the different calibration data used, there are two CSP-LDA-based calibration methods: (1) Motor Imagery Cross-Subject calibration (denoted as MI-CS in Table I): The MI data of the target subject were used as testing data, and the MI data of the source subjects were used as training data. 2) Tactile Cross-Subject calibration (denoted as Tactile-CS in Table I): The MI data of the target subject were used as testing data, and the TS data of the source subjects were used as training data. Moreover, in order to simulate trial-limited scenarios, a subset of the trials was randomly chosen for performance evaluation, and this process was repeated 20 times.

The second calibration algorithm was based on a deep transfer learning model, which leveraged the technology of transfer learning, which is a popular method in computer vision or natural language processing. In transfer learning, there is a pre-trained model that has been trained on large open-source datasets. When the model is used for a specific task, the task-specific data is then used to perform subtle parameter updates through a process known as fine-tuning. This technology has also been validated in MI-based BCI [19], [38]. The deep transfer learning model EEGsym [38] was used in this study. This cross-subject decoding scheme comprises two primary stages: the pre-training stage and the fine-tuning stage. During the pre-training stage, EEG data from

TABLE I
THE DETAIL CALIBRATION CONFIGURATION. NOTE: TACTILE-CS AND TACTILE-CSFT ARE TACTILE CALIBRATION METHODS. MI-CS AND MI-CSFT ARE TRADITIONAL MI CALIBRATION METHODS

Calibration Methods		Training Data	Fine-tuning Data	Testing Data
Traditional MI Calibration	MI-CS	MI data of source subjects	-	MI data of target subject
	MI-CSFT	MI data of the public datasets	MI data of source subjects	
Tactile Calibration	Tactile-CS	TS data of source subjects	-	
	Tactile-CSFT	MI data of the public datasets	TS data of source subjects	

five publicly available datasets (i.e. Physionet [56], OpenBMI [57], Kaya2018 [58], Meng2019 [59], and Stieger2021 [60]), including 280 subjects, were utilized to train the deep learning model EEGSym. For each subject in the pre-training datasets, 10 trials of each class were selected for the validation dataset, with the remainder allocated to the training dataset. The pre-training process was terminated when the validation loss failed to improve for 25 consecutive iterations. In the fine-tuning stage, the pre-trained deep learning model was further fine-tuned using aligned EEG data from our dataset, following the fine-tuning settings in [38]: (1) Early stopping: The fine-tuning process would automatically stop when validation loss did not improve for 25 consecutive iterations. (2) Learning rate: The whole structure was fine-tuned at a very low learning rate (i.e. 0.0001) until the early stopping strategy was triggered. Subsequently, the fine-tuned model was employed to decode the target subject in our dataset. For a more detailed structure of the EEGSym model, we encourage readers to refer to the comprehensive description provided in the referenced paper [38]. Again, according to the different fine-tuning data used, there were two deep transfer learning-based calibration methods: (1) Motor Imagery Cross-Subject Fine-Tuning calibration (denoted as MI-CSFT in Table I): The MI data of the target subject were used as testing data, the MI data of the public datasets were used as training data, and the MI data of the source subjects were used as fine-tuning data. (2) Tactile Cross-Subject Fine-Tuning calibration (denoted as Tactile-CSFT in Table I): The MI data of the target subject were used as testing data, the MI data of the public datasets were used as training data, and the TS data of the source subjects were used as fine-tuning data. Sixteen EEG channels were selected according to the training data of the pre-trained model [38].

A total of four calibration methods were evaluated, which are summarized in Table I. For each performance evaluation, one target subject, whose EEG signals will be testing data, was chosen from the 12 subjects. The remaining 11 subjects were used as source subjects whose EEG signals will be used as the calibration data for the model. Each subject would be the target subject once evaluated by two algorithms with two kinds of calibration data (i.e. MI data and TS data).

III. RESULTS

A. Event-Related Desynchronization Analysis

The TS task and the MI task exhibit similar patterns of cortex activation, providing a neurophysiological basis for using tactile-induced brain patterns to calibrate motor imagery-based

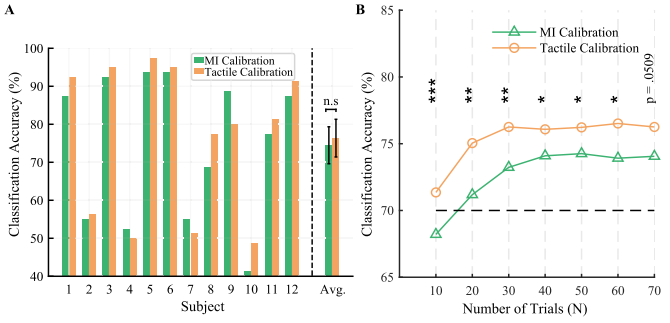

Fig. 2. Cross-subject BCI decoding performance with CSP-LDA algorithm. (A) BCI decoding performance across different calibration methods using all trials. 'n.s' indicates no significant difference in paired t-test. (B) The effect of the number of trials (the sum of trials in two classes) on BCI decoding performance. '*','**', '***', and 'n.s' represent $p < 0.05$, $p < 0.01$, $p < 0.001$ and no significant difference in paired t-test, respectively.

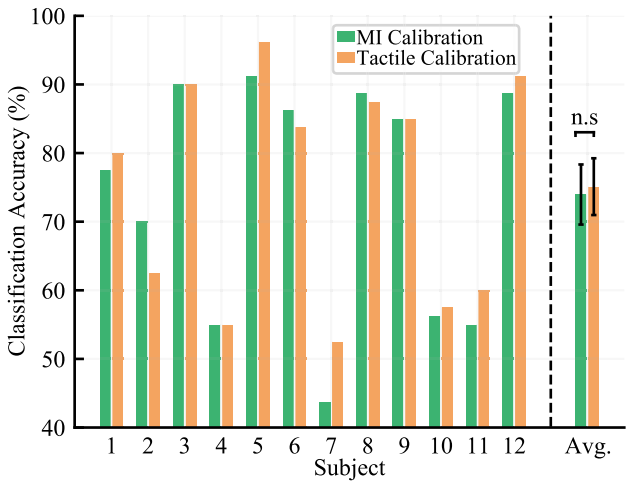

Fig. 3. Cross-subject BCI decoding performance with a pre-trained deep transfer learning model across different calibration methods. 'n.s' indicates no significant difference in paired t-test.

BCIs. Specifically, the cortical activations induced by both tasks are similar in their spatial distribution, as demonstrated in Fig. 4 (A). In both the TS task and the MI task, the ERD/ERS is concentrated over the left and right sensorimotor cortex. Additionally, both tasks show a contralateral phenomenon in their ERD activation, meaning that the ERD activation is situated in the hemisphere opposite to the limb being imagined or stimulated. For example, in the left MI task and the left TS task, the ERD activation is located in the contralateral right hemisphere, while in the right MI task and the right TS task, the ERD activation is located in the contralateral left hemisphere.

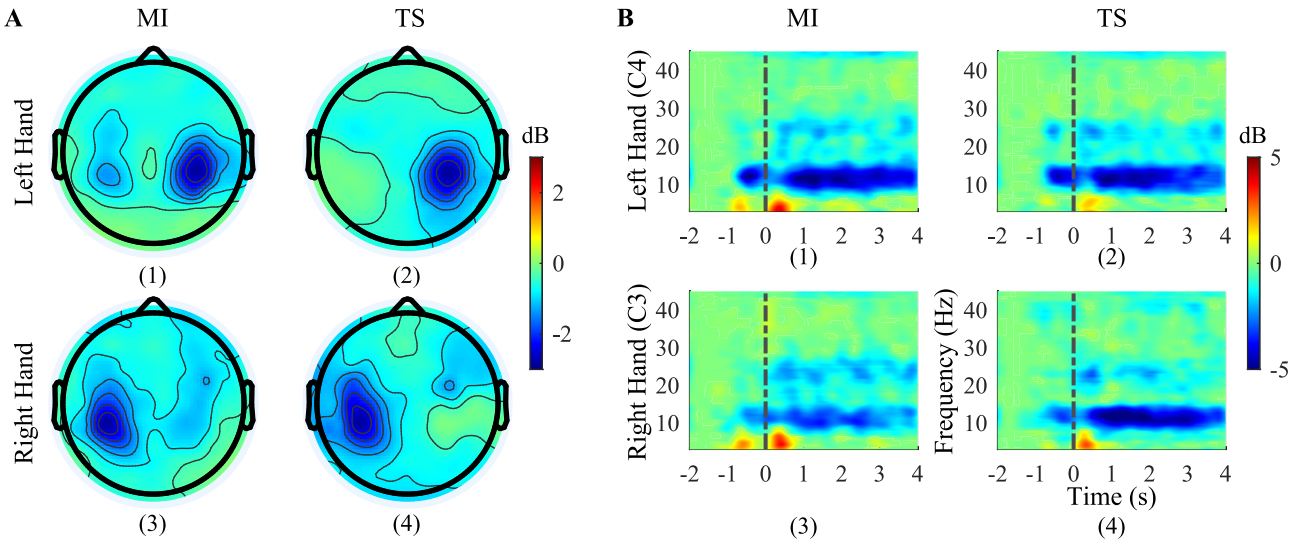

Fig. 4. The grand-averaged ERD/ERS in the spatial domain and the frequency domain. (A) The topoplot of grand-averaged ERD/ERS across different tasks and blocks, which is computed within the alpha-beta band [8 26] Hz and the 1 to 4 s with respect to the appearance of the red cue. (A)(1) and (A)(3) are ERD/ERS patterns of the MI-L task and the MI-R task in the MI block. (A)(2) and (A)(4) are ERD/ERS patterns of the TS-L task and the TS-R task in the TS block. (B) The grand-averaged ERSP value at small Laplace filtered C3 and C4 channels across different tasks and blocks. ERSP for the (1) MI-L task of the C4 channel in the MI block, (2) TS-L task of the C4 channel in the TS block, (3) MI-R task of the C3 channel in the MI block, and (4) TS-R task of the C3 channel in the TS block. The dashed line at time 0 s corresponds to the appearance of the red cue when subjects began to perform the MI or TS tasks.

Furthermore, the cortical activations induced by the MI task and the TS task are also similar in their frequency distribution, as represented by ERSP values. Fig. 4 (B) displays the alpha [8 14] and beta [15 26] bands being activated in the contralateral hemisphere for both the TS task and the MI task (with C3 representing the left hemisphere and C4 representing the right hemisphere). Of particular interest is the observation that the ERD activated by the TS-R task is more pronounced in the alpha band compared to the MI-R task.

B. Motor Imagery Performance Analysis

The results of the CSP-LDA algorithm are presented in Fig. 2 (A). Both calibration methods achieved similar levels of accuracy. In the traditional MI calibration method, the accuracy was 74.48 $\pm$ 18.25%. For the Tactile calibration, the accuracy was 76.35 $\pm$ 18.61%. There was no significant difference between the two methods (paired t-test, $p = 0.2188$). However, as illustrated in Fig. 2 (B), the Tactile calibration demonstrated a significant advantage when the sample size was limited. When the trial number per class was less than 30 for one subject, the accuracy achieved by the Tactile calibration was significantly higher than that of the traditional MI calibration at a significant level of $p < 0.01$. Furthermore, the Tactile calibration required fewer calibration trials to achieve a basic control level of 70% accuracy in BCIs. Specifically, in the Tactile calibration, only five trials per class were needed for one subject (a total of 110 trials), while the traditional MI calibration required at least ten trials per class for one subject (a total of 220 trials).

In practical applications, BCIs often face limitations in the number of available EEG channels, which can impact MI decoding accuracy and reliability. Transfer learning algorithms can address this challenge by leveraging knowledge from other subjects to improve BCI performance. Information from other

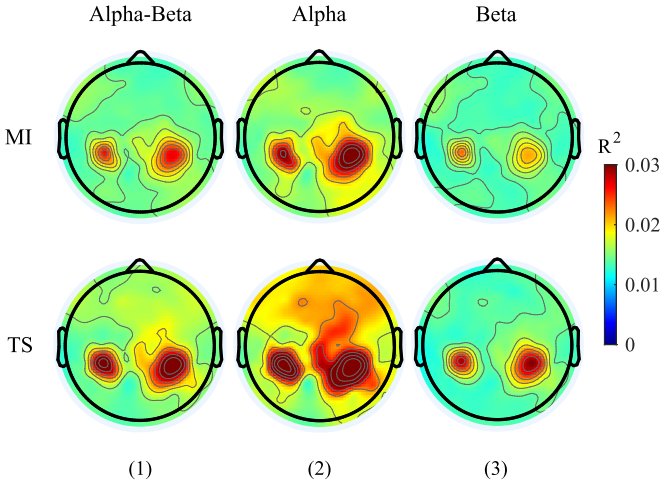

Fig. 5. The spatial distribution of grand-averaged R^2 across different frequency bands. The R^2 was averaged in the 1 to 4 s with respect to the appearance of the red cue in each block. (1) The R^2 distribution within the alpha-beta band [8 26] across different blocks. (2) The R^2 distribution within the alpha band [8 14] across different blocks. (3) The R^2 distribution within the beta band [15 26] across different blocks.

subjects can be transferred to the target subject, enabling more accurate and efficient MI decoding even with a limited number of EEG channels. Thus, we also evaluated the performance of a transfer learning model (i.e., EEGsym) in a 16-channel setup. The Tactile calibration method achieved a similar level of performance as the traditional MI calibration method (73.96 $\pm$ 17.16% vs. 75.10 $\pm$ 16.21%, paired t-test, $p = 0.1794$).

C. Discriminant Information Analysis

R^2 values, serving as indicators of discriminative information, were computed to gain deeper insights into how Tactile calibration enhances BCI performance. Fig. 5 illustrates the grand-averaged spatial distributions of R^2 in the MI task

TABLE II
TIME COST OF DIFFERENT CALIBRATION METHODS IN THE DEEP TRANSFER LEARNING ALGORITHM

	Traditional MI Calibration	Tactile Calibration
Time Cost	426.19 ± 61.00 s	395.72 ± 68.65 s

and the TS task across different frequency bands. The distribution of discriminative information is found to be similar for both tasks, primarily concentrated in the sensorimotor cortex. However, it is noteworthy that the R^2 value for the TS task exceeds that of the MI task across all frequency bands, partially explaining the superior performance achieved by the Tactile calibration method.

Moreover, a comparison was made between the time required for fine-tuning using the Tactile calibration method and the traditional MI calibration method. The results, as shown in Table II, indicate that the deep transfer learning algorithm employed in Tactile calibration achieved the early stop strategy significantly faster than in the conventional MI calibration. This observation suggests that the tactile stimulation data exhibited more distinct and discriminative EEG patterns, leading to a faster convergence speed of the deep transfer learning algorithm.

IV. DISCUSSION

A. Calibration Effectiveness

In this study, the feasibility of cross-subject Motor Imagery (MI) calibration using tactile Event-Related Desynchronization (ERD) was validated with different algorithms. The proposed calibration method was compared with the traditional MI calibration method. The results revealed that the proposed calibration method achieved a similar level of performance as the traditional MI calibration method. Particularly, when the number of trials was limited, the proposed method demonstrated significantly higher performance compared to the traditional MI calibration method. To validate the effectiveness of the tactile data training model, a comprehensive performance evaluation was further conducted on several state-of-the-art algorithms, including basic Common Spatial Pattern-Linear Discriminant Analysis (CSP-LDA) (i.e., CSP-LDA without data alignment), MEKT [32], EEGNet [35], and DeepConvNet [37]. As depicted in Table III, the proposed tactile cross-subject calibration method demonstrated comparable performance to the traditional MI calibration method. These results are particularly promising, considering that in the tactile ERD-based calibration approach, no motor imagery data is needed.

B. Similar ERD in MI and TS Tasks

In our study, as depicted in Fig. 4, tactile stimuli elicited prominent ERD, primarily concentrated in the sensorimotor cortex of the contralateral cerebral hemisphere, which is consistent with the previous studies [61]. This pattern closely resembled the ERD induced by motor imagery. Two potential reasons may account for this observed similarity. Firstly, it may be attributed to the joint activation mechanism of the sensorimotor cortex [62]. The sensory cortex and the motor cortex, besides being spatially proximate, tend to exhibit neural firing concurrently [63], given that physical movement typically triggers sensory input. Consequently, these cortices exhibit a robust neural interconnection wherein the activation of one can induce concurrent activation of the other. Previous research has demonstrated that motor imagery involves activation not only in the primary motor cortex (M1) but also in the primary somatosensory cortex (S1) [64], even in the absence of tactile input. Therefore, the tactile stimulation used in our method might activate both S1 and M1 areas [65], elucidating the nearly identical ERD patterns induced by the TS task and MI task. Another plausible explanation for the similarity in the ERDs induced by motor imagery and tactile stimulation lies in the spatial resolution limitations imposed by EEG equipment, combined with the spatial proximity of the sensory cortex and the motor cortex. This limitation renders it challenging to distinguish between the two distributions of ERD. Despite employing a high-density EEG device, discerning significant differences in the activation of brain areas between the MI task and the TS task proved elusive. Consequently, the data generated by these two tasks may share a similar data distribution. This alignment holds significant importance in the context of supervised machine learning, ensuring that the training and testing data match each other, constituting a pivotal factor for successful calibration.

C. Comparasion With Previous Methods for Relieving Calibration Workload

Relieving the workload of BCI calibration has attracted extensive research interest. The existing work shows that active movement [15], passive movement [16], and electrical stimulation can all induce ERD patterns similar to MI, and can be used for the calibration of MI [17]. In our calibration method, tactile stimuli were applied to the wrists of the subjects by two wearable motors, about the size of a quarter of a coin. Compared with the passive movement calibration method, our device is more portable and does not require the assistance of a robot. Furthermore, individuals who have undergone amputation can no longer utilize the calibration methods for both active and passive movement. Despite this, their sensory input channels remain intact after the amputation, indicating that our calibration method may serve as a superior replacement. Our tactile stimulation is applied to the skin in the form of mechanical vibration and does not involve electrical current stimulation. As a result, it remains unaffected by current artifacts. Conversely, the calibration method that relies on electrical stimulation runs the risk of inducing artifacts, as stated in [18]. Furthermore, none of the aforementioned studies focus on the cross-subject decoding scenario. It remains an area of interest to investigate whether the patterns of ERD/ERS variations observed in the aforementioned studies are consistent with MI across different subjects. In our calibration method, we conducted an evaluation of cross-subject performance and discovered a strong correlation (Pearson correlation, $r = 0.97$, $p < 0.0001$) between Tactile calibration and traditional MI calibration, as depicted in Fig. 6. This finding suggests that the variations in tactile-induced ERD and MI-induced ERD may be similar

TABLE III
CROSS-SUBJECT BCI DECODING PERFORMANCE ACROSS ALGORITHMS AND CALIBRATION METHODS

Calibration Method	Basic CSP-LDA (%)	MEKT (%)	EEGNet (%)	DeepConvNet (%)
Traditional MI Calibration	66.56 ± 15.43	72.19 ± 17.62	64.79 ± 15.81	**64.47 ± 12.61**
Tactile Calibration	**68.44 ± 16.93**	**74.79 ± 14.29**	**70.42 ± 15.55**	63.85 ± 13.79

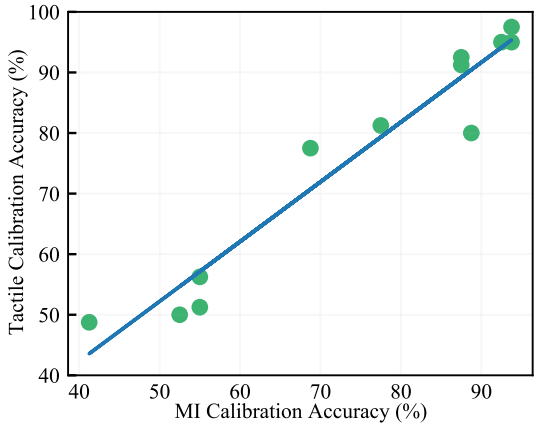

Fig. 6. Pearson correlation between Tactile calibration performance and traditional MI calibration performance. Each subject is represented as a green circle, and the linear polynomial is used for regression based on a least square regression fit.

among subjects, thereby highlighting the feasibility of utilizing Tactile calibration in the cross-subject scenario.

To mitigate the calibration workload associated with MI-based BCI, transfer learning has also been extensively explored [19]. In early studies, researchers primarily conducted knowledge transfer between different subjects [28], [32], [35] or sessions [20], [66], utilizing data from diverse subjects or sessions (source domain) to train models for decoding data from the target subject or session (target domain). Recent advancements extend this to knowledge transfer between different datasets [38], even those collected by different devices, termed as cross-device transfer learning [24]. Notably, He and Wu [23] proposed knowledge transfer between distinct tasks, exemplified by data in the source domain originating from left and right-hand MI tasks and the target domain data consisting of tasks of feet and tongue motor imagery. However, due to the distinct brain activation patterns associated with hand, feet, and tongue MI tasks [67], cross-task transfer learning may lack intuitive coherence. In this study, we also conducted knowledge transfer between different tasks, specifically tactile stimulation task and motor imagery task. As depicted in Fig. 4, tactile stimulation induces brain activation patterns similar to motor imagery, facilitating knowledge transfer. While the primary aim of applying transfer learning in BCI is to tackle the challenge of limited data in the target subject, a crucial step involves employing domain adaptation methods to align target domain data with that of the source domain or fine-tuning a pre-trained model on the source domain to decode target domain data [68]. This typically requires data from subjects in the target domain, whether labeled or unlabeled [21]. Thus, many existing transfer learning methods still demand motor imagery data from the target subject for the domain adaptation process [21]. However, given the non-stationary nature [11] and the low signal-to-noise ratio of motor imagery data [12], the need for fine-tuning data increases, contradicting the original purpose of utilizing transfer learning in BCI. In contrast, our approach involves only using tactile stimulation-induced data for fine-tuning the pre-trained model or directly training a classifier, as opposed to using motor imagery data. This innovative strategy aims to achieve the noteworthy goal of zero motor imagery samples requirement for the target subject. As illustrated in Fig. 3, the EEGSym results indicate that data induced by tactile stimulation can be effectively used to fine-tune models pre-trained on motor imagery-induced data.

D. Potential Applications

The results of the current study hold potential significance in cross-population decoding scenarios. For example, in the case of MI decoding for the elderly population, collecting calibration data is often challenging due to the limited energy [69]. By utilizing data passively induced by tactile stimulation as fine-tuning data for models trained on motor imagery-induced data from young adults, direct decoding can be achieved without the need to collect MI data. Moreover, as a convenient and effective MI calibration method, it may have more extensive application potential in clinical practice. Passive tactile stimulation is input from the outside and can be controlled in real-time and accurately. It may be less susceptible to interference by the subjects' internal task-unrelated mental state (e.g. attention deficit patients have difficulty concentrating their attention) than the MI task, which is a completely spontaneous internal activity of the subjects. As shown in Fig. 5, the ERD induced by tactile stimulation has more discriminant information in both the alpha and the beta band, which means data with higher quality was obtained in the TS task. In the clinical application of stroke rehabilitation, the starting stage of rehabilitation training is difficult [70], mainly because doctors have difficulty making sure that patients have made correct actions, and some patients have communication difficulties or have difficulty understanding the abstract MI tasks. However, the tactile stimulation can be completely controlled by the doctor, which can help to quickly collect calibration data and begin the feedback rehabilitation training process faster. In other applications of BCI, such as automatic driving [71], [72] and multitask game [73], it may be difficult for users to focus their attention on the MI task, because they need to allocate their attention to other tasks at the same time. Tactile stimulation provides a passive alternative that requires less workload and can improve the user experience of brain-computer interfaces.

E. Limitations

The limitation of our study is that we did not evaluate online performance because we focused on cross-subject calibration, where data from all subjects were collected before

performance evaluation. For practical applications, online performance should be evaluated in the future. First, we need to build a database of EEG data induced by tactile stimulation and train a deep transfer learning model. Then transfer learning technology will be used to fine-tune the pre-trained model to the target user and achieve real-time decoding. Additionally, it would be worthwhile to investigate whether the proposed method can achieve comparable decoding performance in the elderly population, considering the decreased tactile sensitivity observed in this demographic [74].

V. Conclusion

In this study, we introduced an innovative cross-subject calibration method for MI-based BCI systems. This approach leverages transfer learning models calibrated using tactile stimulation-induced ERD to decode motor imagery data. Our proposed method achieves decoding performance comparable to the traditional MI calibration method. Notably, the proposed calibration method outperforms the traditional MI calibration with fewer trials. The tactile method utilizes passive afferent tactile stimulation, which is measurable, controllable, and easy to implement. This makes it highly promising for practical applications of BCI, particularly in clinical settings.

Acknowledgment

The authors would like to thank all volunteers for their participation in the study.

References

[1] J. R. Wolpaw, N. Birbaumer, D. J. McFarland, G. Pfurtscheller, and T. M. Vaughan, "Brain–computer interfaces for communication and control," *Clin. Neurophysiol.*, vol. 113, no. 6, pp. 767–791, Jun. 2002.

[2] A. R. Murguialday et al., "Transition from the locked in to the completely locked-in state: A physiological analysis," *Clin. Neurophysiol.*, vol. 122, no. 5, pp. 925–933, May 2011.

[3] X. Gu et al., "EEG-based brain–computer interfaces (BCIs): A survey of recent studies on signal sensing technologies and computational intelligence approaches and their applications," *IEEE/ACM Trans. Comput. Biol. Bioinf.*, vol. 18, no. 5, pp. 1645–1666, Sep. 2021.

[4] L. A. Farwell and E. Donchin, "Talking off the top of your head: Toward a mental prosthesis utilizing event-related brain potentials," *Electroencephalogr. Clin. Neurophysiol.*, vol. 70, no. 6, pp. 510–523, Dec. 1988.

[5] M. Cheng, X. Gao, S. Gao, and D. Xu, "Design and implementation of a brain–computer interface with high transfer rates," *IEEE Trans. Biomed. Eng.*, vol. 49, no. 10, pp. 1181–1186, Oct. 2002.

[6] G. Pfurtscheller, C. Neuper, D. Flotzinger, and M. Pregenzer, "EEG-based discrimination between imagination of right and left hand movement," *Electroencephalogr. Clin. Neurophysiol.*, vol. 103, pp. 642–651, Dec. 1997.

[7] J. Meng, S. Zhang, A. Bekyo, J. Olsoe, B. Baxter, and B. He, "Non-invasive electroencephalogram based control of a robotic arm for reach and grasp tasks," *Sci. Rep.*, vol. 6, no. 1, p. 38565, Dec. 2016.

[8] N. Mrachacz-Kersting et al., "Efficient neuroplasticity induction in chronic stroke patients by an associative brain–computer interface," *J. Neurophysiol.*, vol. 115, no. 3, pp. 1410–1421, Mar. 2016.

[9] C. Jeunet, E. Jahanpour, and F. Lotte, "Why standard brain–computer interface (BCI) training protocols should be changed: An experimental study," *J. Neural Eng.*, vol. 13, no. 3, Jun. 2016, Art. no. 036024.

[10] G. Pfurtscheller and C. Neuper, "Motor imagery and direct brain–computer communication," *Proc. IEEE*, vol. 89, no. 7, pp. 1123–1134, Jul. 2001.

[11] Y. Shin, S. Lee, M. Ahn, H. Cho, S. C. Jun, and H.-N. Lee, "Noise robustness analysis of sparse representation based classification method for non-stationary EEG signal classification," *Biomed. Signal Process. Control*, vol. 21, pp. 8–18, Aug. 2015.

[12] L. F. Nicolas-Alonso and J. Gomez-Gil, "Brain computer interfaces, a review," *Sensors*, vol. 12, no. 2, pp. 1211–1279, Jan. 2012.

[13] C. Vidaurre, C. Sannelli, K.-R. Müller, and B. Blankertz, "Co-adaptive calibration to improve BCI efficiency," *J. Neural Eng.*, vol. 8, no. 2, Apr. 2011, Art. no. 025009.

[14] A. Singh, A. A. Hussain, S. Lal, and H. W. Guesgen, "A comprehensive review on critical issues and possible solutions of motor imagery based electroencephalography brain–computer interface," *Sensors*, vol. 21, no. 6, p. 2173, Mar. 2021.

[15] V. Kaiser, A. Kreilinger, G. Mueller-Putz, and C. Neuper, "First steps toward a motor imagery based stroke BCI: New strategy to set up a classifier," *Frontiers Neurosci.*, vol. 5, p. 86, Jul. 2011.

[16] G. R. Müller-Putz, D. Zimmermann, B. Graimann, K. Nestinger, G. Korisek, and G. Pfurtscheller, "Event-related beta EEG-changes during passive and attempted foot movements in paraplegic patients," *Brain Res.*, vol. 1137, pp. 84–91, Mar. 2007.

[17] C. Vidaurre et al., "Neuromuscular electrical stimulation induced brain patterns to decode motor imagery," *Clin. Neurophysiol.*, vol. 124, no. 9, pp. 1824–1834, Sep. 2013.

[18] U. Hoffmann, W. Cho, A. Ramos-Murguialday, and T. Keller, "Detection and removal of stimulation artifacts in electroencephalogram recordings," in *Proc. Annu. Int. Conf. IEEE Eng. Med. Biol. Soc.*, Aug. 2011, pp. 7159–7162.

[19] D. Wu, Y. Xu, and B.-L. Lu, "Transfer learning for EEG-based brain–computer interfaces: A review of progress made since 2016," *IEEE Trans. Cognit. Develop. Syst.*, vol. 14, no. 1, pp. 4–19, Mar. 2022.

[20] K. Zhang, N. Robinson, S.-W. Lee, and C. Guan, "Adaptive transfer learning for EEG motor imagery classification with deep convolutional neural network," *Neural Netw.*, vol. 136, pp. 1–10, Apr. 2021.

[21] D. Wu, X. Jiang, and R. Peng, "Transfer learning for motor imagery based brain–computer interfaces: A tutorial," *Neural Netw.*, vol. 153, pp. 235–253, Sep. 2022.

[22] X. Si, H. He, J. Yu, and D. Ming, "Cross-subject emotion recognition brain–computer interface based on fNIRS and DBJNet," *Cyborg Bionic Syst.*, vol. 4, p. 0045, Jan. 2023.

[23] H. He and D. Wu, "Different set domain adaptation for brain–computer interfaces: A label alignment approach," *IEEE Trans. Neural Syst. Rehabil. Eng.*, vol. 28, no. 5, pp. 1091–1108, May 2020.

[24] L. Xu, M. Xu, Y. Ke, X. An, S. Liu, and D. Ming, "Cross-dataset variability problem in EEG decoding with deep learning," *Frontiers Hum. Neurosci.*, vol. 14, p. 103, Apr. 2020.

[25] I. Hossain, A. Khosravi, I. Hettiarachchi, and S. Nahavandi, "Multiclass informative instance transfer learning framework for motor imagery-based brain–computer interface," *Comput. Intell. Neurosci.*, vol. 2018, Feb. 2018, Art. no. 6323414.

[26] V. Jayaram, M. Alamgir, Y. Altun, B. Scholkopf, and M. Grosse-Wentrup, "Transfer learning in brain–computer interfaces," *IEEE Comput. Intell. Mag.*, vol. 11, no. 1, pp. 20–31, Feb. 2016.

[27] H. Albalawi and X. Song, "A study of kernel CSP-based motor imagery brain computer interface classification," in *Proc. IEEE Signal Process. Med. Biol. Symp. (SPMB)*, Dec. 2012, pp. 1–4.

[28] M. Dai, D. Zheng, S. Liu, and P. Zhang, "Transfer kernel common spatial patterns for motor imagery brain–computer interface classification," *Comput. Math. Methods Med.*, vol. 2018, Mar. 2018, Art. no. 9871603.

[29] F. Lotte and C. Guan, "Learning from other subjects helps reducing brain–computer interface calibration time," in *Proc. IEEE Int. Conf. Acoust., Speech Signal Process.*, Mar. 2010, pp. 614–617.

[30] A. M. Azab, L. Mihaylova, K. K. Ang, and M. Arvaneh, "Weighted transfer learning for improving motor imagery-based brain–computer interface," *IEEE Trans. Neural Syst. Rehabil. Eng.*, vol. 27, no. 7, pp. 1352–1359, Jul. 2019.

[31] P. L. C. Rodrigues, C. Jutten, and M. Congedo, "Riemannian Procrustes analysis: Transfer learning for brain–computer interfaces," *IEEE Trans. Biomed. Eng.*, vol. 66, no. 8, pp. 2390–2401, Aug. 2019.

[32] W. Zhang and D. Wu, "Manifold embedded knowledge transfer for brain–computer interfaces," *IEEE Trans. Neural Syst. Rehabil. Eng.*, vol. 28, no. 5, pp. 1117–1127, May 2020.

[33] P. Zanini, M. Congedo, C. Jutten, S. Said, and Y. Berthoumieu, "Transfer learning: A Riemannian geometry framework with applications to brain–computer interfaces," *IEEE Trans. Biomed. Eng.*, vol. 65, no. 5, pp. 1107–1116, May 2018.

[34] H. He and D. Wu, "Transfer learning for brain–computer interfaces: A Euclidean space data alignment approach," *IEEE Trans. Biomed. Eng.*, vol. 67, no. 2, pp. 399–410, Feb. 2020.

[35] V. Lawhern, A. Solon, N. Waytowich, S. Gordon, C. Hung, and B. Lance, "EEGNet: A compact convolutional neural network for EEG-based brain–computer interfaces," *J. Neural Eng.*, vol. 15, Nov. 2016, Art. no. 056013.

[36] R. Mane et al., "FBCNet: A multi-view convolutional neural network for brain–computer interface," 2021, *arXiv:2104.01233*.

[37] R. T. Schirrmeister et al., "Deep learning with convolutional neural networks for EEG decoding and visualization," *Hum. Brain Mapping*, vol. 38, no. 11, pp. 5391–5420, Nov. 2017.

[38] S. Pérez-Velasco, E. Santamaría-Vázquez, V. Martínez-Cagigal, D. Marcos-Martínez, and R. Hornero, "EEGSym: Overcoming inter-subject variability in motor imagery based BCIs with deep learning," *IEEE Trans. Neural Syst. Rehabil. Eng.*, vol. 30, pp. 1766–1775, 2022.

[39] F. Zhuang et al., "A comprehensive survey on transfer learning," *Proc. IEEE*, vol. 109, no. 1, pp. 43–76, Jan. 2021.

[40] G. Huang et al., "Discrepancy between inter- and intra-subject variability in EEG-based motor imagery brain–computer interface: Evidence from multiple perspectives," *Frontiers Neurosci.*, vol. 17, Feb. 2023, Art. no. 1122661.

[41] S. Saha, K. I. U. Ahmed, R. Mostafa, L. Hadjileontiadis, and A. Khandoker, "Evidence of variabilities in EEG dynamics during motor imagery-based multiclass brain–computer interface," *IEEE Trans. Neural Syst. Rehabil. Eng.*, vol. 26, no. 2, pp. 371–382, Feb. 2018.

[42] D. Zha et al., "Data-centric artificial intelligence: A survey," 2023, *arXiv:2303.10158*.

[43] A.-M. Brouwer and J. Van Erp, "A tactile P300 brain–computer interface," *Frontiers Neurosci.*, vol. 4, p. 1440, May 2010.

[44] S. Ahn, M. Ahn, H. Cho, and S. C. Jun, "Achieving a hybrid brain–computer interface with tactile selective attention and motor imagery," *J. Neural Eng.*, vol. 11, no. 6, Dec. 2014, Art. no. 066004.

[45] A. Chatterjee, V. Aggarwal, A. Ramos, S. Acharya, and N. V. Thakor, "A brain–computer interface with vibrotactile biofeedback for haptic information," *J. Neuroeng. Rehabil.*, vol. 4, no. 1, p. 40, Oct. 2007.

[46] L. Yao, J. Meng, D. Zhang, X. Sheng, and X. Zhu, "Selective sensation based brain–computer interface via mechanical vibrotactile stimulation," *PLoS ONE*, vol. 8, no. 6, Jun. 2013, Art. no. e64784.

[47] L. Yao, J. Meng, D. Zhang, X. Sheng, and X. Zhu, "Combining motor imagery with selective sensation toward a hybrid-modality BCI," *IEEE Trans. Biomed. Eng.*, vol. 61, no. 8, pp. 2304–2312, Aug. 2014.

[48] C. Thyrion and J.-P. Roll, "Perceptual integration of illusory and imagined kinesthetic images," *J. Neurosci.*, vol. 29, no. 26, pp. 8483–8492, Jul. 2009.

[49] Y. Zhong, L. Yao, J. Wang, and Y. Wang, "Tactile sensation assisted motor imagery training for enhanced BCI performance: A randomized controlled study," *IEEE Trans. Biomed. Eng.*, vol. 70, no. 2, pp. 694–702, Feb. 2023.

[50] L. Yao, M. Jianjun, X. Sheng, D. Zhang, and X. Zhu, "A novel calibration and task guidance framework for motor imagery BCI via a tendon vibration induced sensation with kinesthesia illusion," *J. Neural Eng.*, vol. 12, Dec. 2014, Art. no. 016005.

[51] J. Wang et al., "Enhanced generalization performance for motor imagery BCI via sensory stimulation," in *Proc. 27th Int. Conf. Mechatronics Mach. Vis. Pract. (M2VIP)*, 2021, pp. 429–434.

[52] B. Blankertz, R. Tomioka, S. Lemm, M. Kawanabe, and K.-R. Müller, "Optimizing spatial filters for robust EEG single-trial analysis," *IEEE Signal Process. Mag.*, vol. 25, no. 1, pp. 41–56, Jan. 2008.

[53] C. Breitwieser, V. Kaiser, C. Neuper, and G. R. Müller-Putz, "Stability and distribution of steady-state somatosensory evoked potentials elicited by vibro-tactile stimulation," *Med. Biol. Eng. Comput.*, vol. 50, no. 4, pp. 347–357, Apr. 2012.

[54] A. Delorme and S. Makeig, "EEGLAB: An open source toolbox for analysis of single-trial EEG dynamics including independent component analysis," *J. Neurosci. Methods*, vol. 134, no. 1, pp. 9–21, Mar. 2004.

[55] M. Tangermann et al., "Review of the BCI competition IV," *Frontiers Neurosci.*, vol. 6, p. 55, Jul. 2012, doi: 10.3389/fnins.2012.00055.

[56] A. L. Goldberger et al., "Physiobank, physiotoolkit, and physionet: Components of a new research resource for complex physiologic signals," *Circulation*, vol. 101, no. 23, pp. E215–E220, Jun. 2000.

[57] M.-H. Lee et al., "EEG dataset and OpenBMI toolbox for three BCI paradigms: An investigation into BCI illiteracy," *GigaScience*, vol. 8, Jan. 2019, Art. no. giz002.

[58] M. Kaya, M. K. Binli, E. Ozbay, H. Yanar, and Y. Mishchenko, "A large electroencephalographic motor imagery dataset for electroencephalographic brain computer interfaces," *Sci. Data*, vol. 5, no. 1, Oct. 2018, Art. no. 180211.

[59] J. Meng and B. He, "Exploring training effect in 42 human subjects using a non-invasive sensorimotor rhythm based online BCI," *Frontiers Hum. Neurosci.*, vol. 13, p. 128, Apr. 2019.

[60] J. R. Stieger, S. Engel, H. Jiang, C. C. Cline, M. J. Kreitzer, and B. He, "Mindfulness improves brain–computer interface performance by increasing control over neural activity in the alpha band," *Cerebral Cortex*, vol. 31, no. 1, pp. 426–438, Jan. 2021.

[61] L. Yao, X. Sheng, N. Mrachacz-Kersting, X. Zhu, D. Farina, and N. Jiang, "Decoding covert somatosensory attention by a BCI system calibrated with tactile sensation," *IEEE Trans. Biomed. Eng.*, vol. 65, no. 8, pp. 1689–1695, Aug. 2018.

[62] K. Kilteni, B. J. Andersson, C. Houborg, and H. H. Ehrsson, "Motor imagery involves predicting the sensory consequences of the imagined movement," *Nature Commun.*, vol. 9, no. 1, p. 1617, Apr. 2018.

[63] D. O. Hebb, Ed., *The Organization of Behavior: A Neuropsychological Theory*. New York, NY, USA: Psychology Press, May 2002.

[64] C. A. Porro et al., "Primary motor and sensory cortex activation during motor performance and motor imagery: A functional magnetic resonance imaging study," *J. Neurosci.*, vol. 16, no. 23, pp. 7688–7698, Dec. 1996.

[65] W. Gaetz and D. Cheyne, "Localization of sensorimotor cortical rhythms induced by tactile stimulation using spatially filtered MEG," *NeuroImage*, vol. 30, no. 3, pp. 899–908, Apr. 2006.

[66] J. Wang, L. Yao, and Y. Wang, "IFNet: An interactive frequency convolutional neural network for enhancing motor imagery decoding from EEG," *IEEE Trans. Neural Syst. Rehabil. Eng.*, vol. 31, pp. 1900–1911, 2023.

[67] G. Pfurtscheller, C. Brunner, A. Schlögl, and F. H. Lopes da Silva, "Mu rhythm (de)synchronization and EEG single-trial classification of different motor imagery tasks," *NeuroImage*, vol. 31, no. 1, pp. 153–159, May 2006.

[68] Z. Wan, R. Yang, M. Huang, N. Zeng, and X. Liu, "A review on transfer learning in EEG signal analysis," *Neurocomputing*, vol. 421, pp. 1–14, Jan. 2021.

[69] M. L. Chen, D. Fu, J. Boger, and N. Jiang, "Age-related changes in vibro-tactile EEG response and its implications in BCI applications: A comparison between older and younger populations," *IEEE Trans. Neural Syst. Rehabil. Eng.*, vol. 27, no. 4, pp. 603–610, Apr. 2019.

[70] S. Silvoni et al., "Brain–computer interface in stroke: A review of progress," *Clin. EEG Neurosci.*, vol. 42, no. 4, pp. 245–252, Oct. 2011.

[71] A. Palumbo, V. Gramigna, B. Calabrese, and N. Ielpo, "Motor-imagery EEG-based BCIs in wheelchair movement and control: A systematic literature review," *Sensors*, vol. 21, no. 18, p. 6285, Sep. 2021.

[72] J. Ju, A. G. Feleke, L. Luo, and X. Fan, "Recognition of drivers' hard and soft braking intentions based on hybrid brain-computer interfaces," *Cyborg Bionic Syst.*, vol. 2022, 2022, doi: 10.34133/2022/9847652.

[73] Z. Wang, Y. Yu, M. Xu, Y. Liu, E. Yin, and Z. Zhou, "Towards a hybrid BCI gaming paradigm based on motor imagery and SSVEP," *Int. J. Hum.–Comput. Interact.*, vol. 35, no. 3, pp. 197–205, Feb. 2019.

[74] J. M. Thornbury and C. M. Mistretta, "Tactile sensitivity as a function of age1," *J. Gerontol.*, vol. 36, no. 1, pp. 34–39, Jan. 1981.